Coastal Dynamics 2017
Paper No. 149

SHORELINE VARIABILITIES OBSERVED AT TWO LOCATIONS IN A LITTORAL CELL

Satoshi Takewaka[1]and Wen Tianue[2]

Abstract

In this observational study, shoreline positions measured at two locations in a littoral cell with X-band radars are shown. The area, southern Kashima Coast, Japan, is an almost a straight sandy coast approximately 17 km long with Hasaki Fishery Port at the south end and Kashima Port at the north end. The radar captures hourly shoreline positions over 4 to 5 km with a spatial resolution of approximately 10 m. The shoreline positions were digitized manually from the radar images with a time interval of few days from year 2010 to 2014. The beach at the research pier HORS can be considered as close to a natural state, where the beach at the southern end of the coast is protected with five Headlands. Spatial and temporal shoreline variabilities, characteristics of long-term trends and seasonal variations of the five years are discussed with the variation of the wave field.

Key words: shoreline variability, wave energy flux, X-band radar

1. Introduction

Monitoring of shoreline positions is essential for proper beach management. Typical traditional methods are surveying, aerial photographing and visible satellite imaging. They are used in many studies to measure shoreline positions, and their performances are well understood. Shortcoming of these methods is low temporal resolution limited by high costs and weather condition. In this context, land based X-band radars are employed at many sites to observe nearshore waves and morphologies continuously in time over several kilometers. They can track long-term, seasonal and rapid shoreline changes, and provide essential data for beach studies. The difficulties of X-band radar observation are limited coverage compared to aerial and satellite imaging, and cost of data processing to extract shoreline position from the radar images.

In this observational study, shoreline positions at two locations in a littoral cell were observed at the southern Kashima Coast, Japan, with two X-band radars as shown in Fig. 1. The area is an almost a straight sandy coast approximately 17 km long with Hasaki Fishery Port at the south end and Kashima Port at the north end, forming a littoral cell. Radar 1 is placed at the research pier HORS of Port and Airport Research Institute, and Radar 2 is placed on a waste treatment plant on the backshore. Single radar captures hourly shoreline positions over 4 to 5 km with a spatial resolution of approximately 10 m as shown in Fig. 2 (a) and (b). The shoreline positions were digitized manually from the radar images with a time interval of few days from year 2010 to 2014.

The beach at the research pier HORS can be considered as close to a natural state. On the contrary, the beach at the southern end of the coast is protected with five Headlands, jetty-like coastal structure. Here, spatial and temporal shoreline variabilities observed at these two locations for the five years are discussed with the variation of the wave field. Recently, Banno et al (2017) report that the shoreline positions of this area is accumulating remarkably, 70 m in the past 50 years on average, due to huge amount of sand damping (approximately 50×10^6 m^3) of excavation of Kashima Port. The result of Radar 2 is consistent with this report, showing rapid accretion at the end of the beach. The wave climate of this area differs in summer and winter: southern waves are observed frequently in summer season, and northern waves in winter.

[1]Department of Engineerign Mechanics and Energy, University of Tsukuba, Tsukuba, Japan.
takewaka@kz.tsukuba.ac.jp
[2]Ditto, 499810784@qq.com

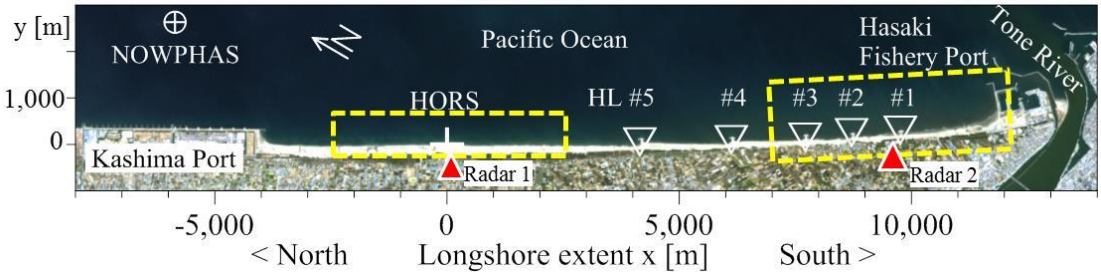

Figure 1. Kashima Coast. ▲Radar location. ▽ Headland (HL, 1-5). NOWPHAS: wave station of Kashima port. The origin of the coordinate system is located at the base of the research pier HORS. Radar 1 is placed on the roof of the research facility of HORS, and Radar 2 on the roof of a waste treatment. The rectangular boxes with yellow dashed lines are the coverage of the radars.

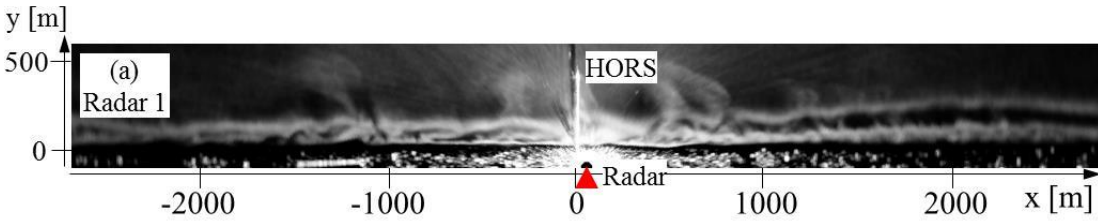

(a)

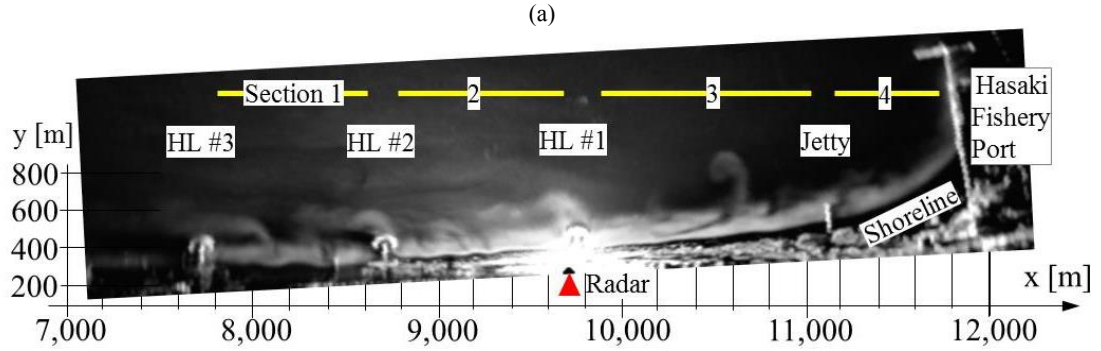

(b)

Figure 2. Radar images and local coordinates. (a) Radar 1 at the research pier HORS (length = 400 m), (b) Radar 2. HL = Headland

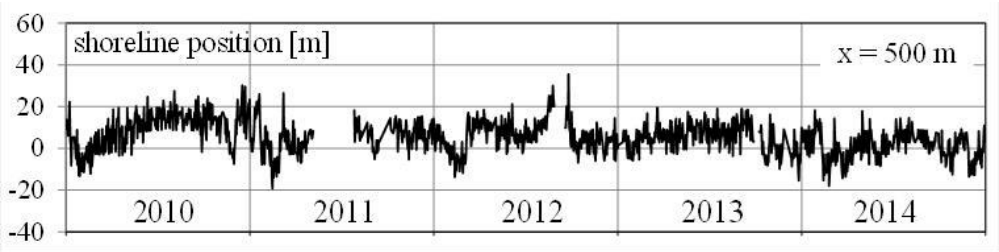

Figure 3. Variation of shoreline position observed at x = 500 m.

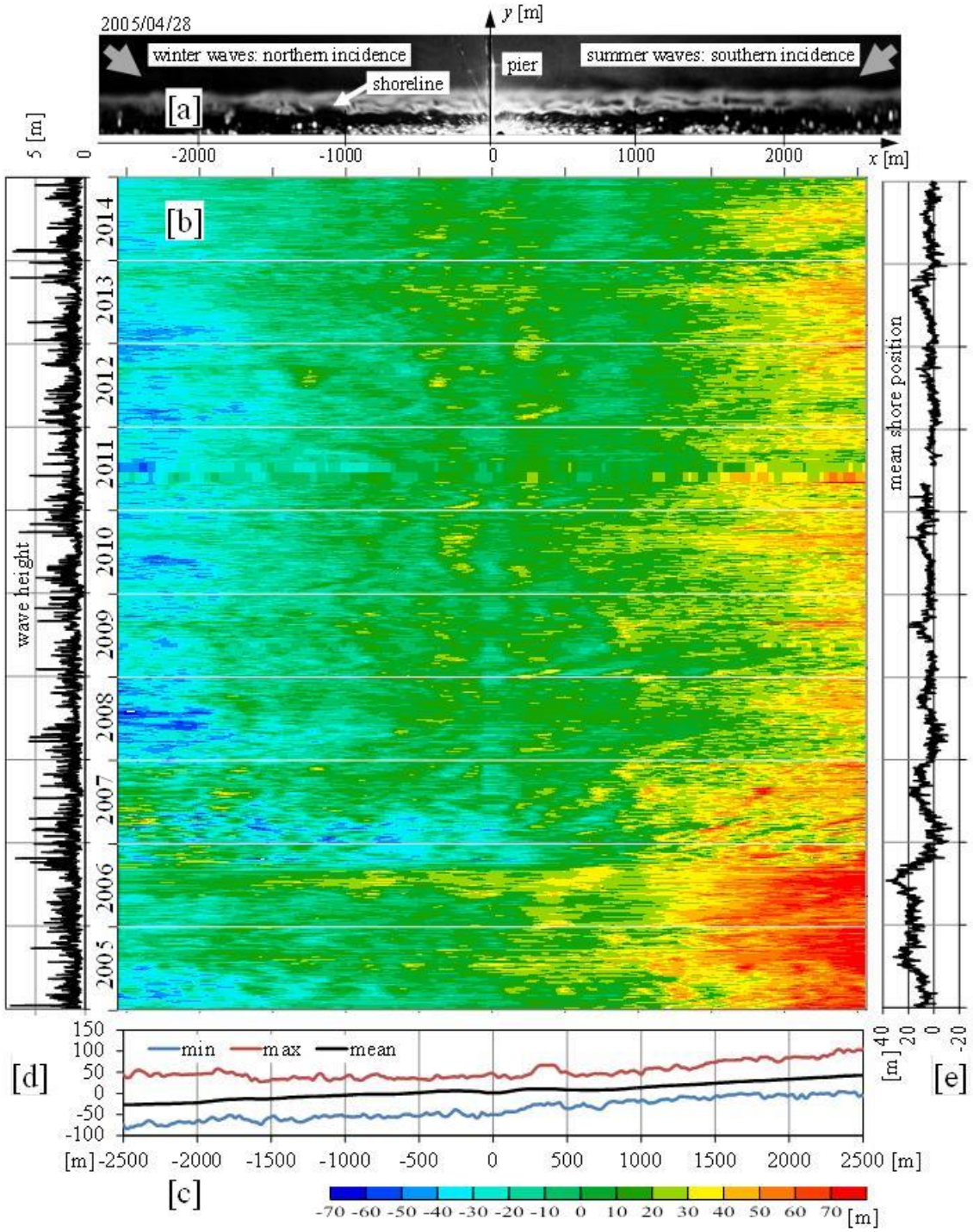

Figure 4. Variation of shoreline position measured at the research pier HORS. (a) Time averaged radar image and local coordinate. (b) Shoreline positions. Lateral is the spatial extent, and vertical is the temporal. (c) mean, maximum and minimum shoreline position during the observation period. (d) Wave height measured at the NOWPHAS of Kashima port (x = -6,000 m). (e) Variation of mean shoreline position.

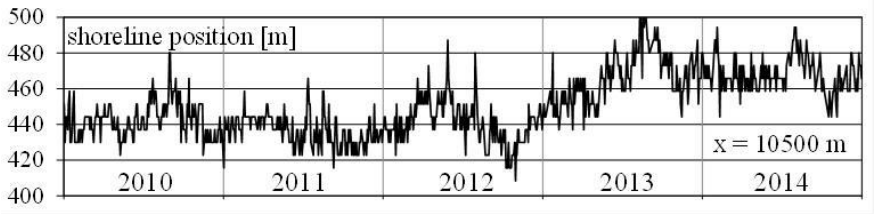

Figure 5. Variation of shoreline position measured at x = 10,500 m.

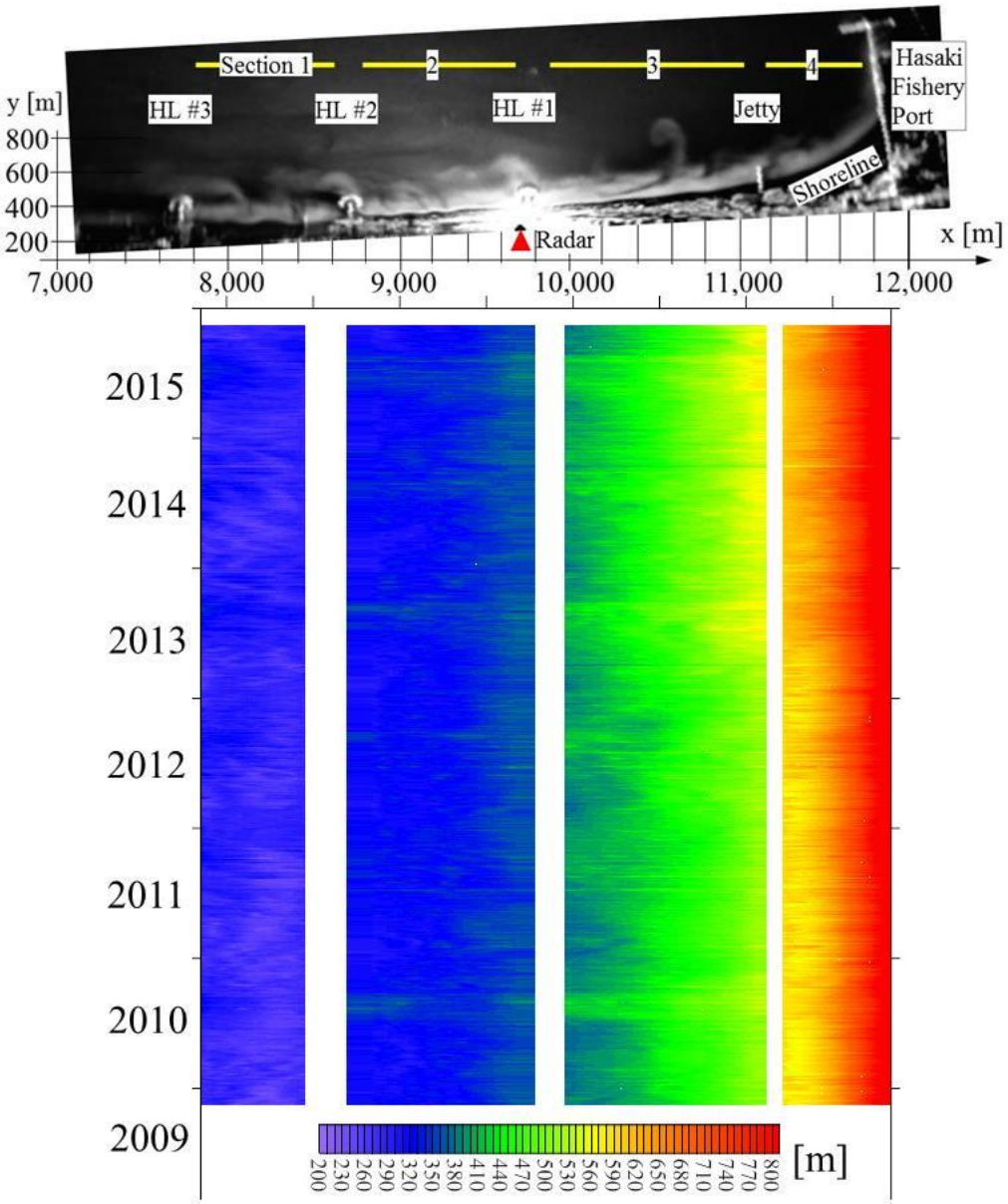

Figure 6. Upper panel shows the time averaged radar image with the coordinate system. This area is divided into Section 1 to 4 to discuss the characteristics of local beach deformation. Lower panel shows the overall variation of shoreline position measured with Radar 2. Lateral is the spatial extent, and vertical is the temporal. The white stripes are the areas where the shoreline positions were not able to digitize due the headlands and jetty.

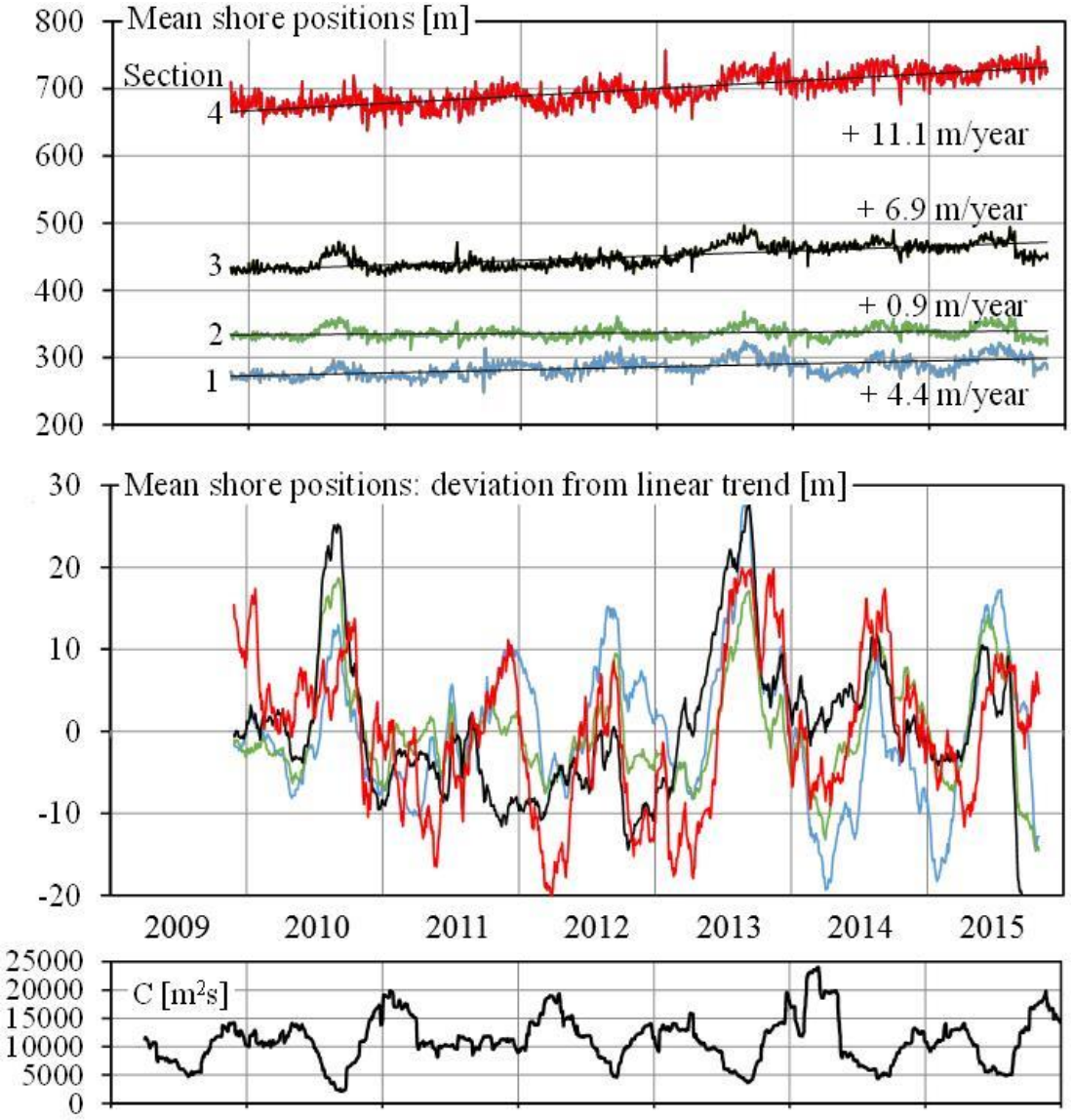

Figure 7. Variation of mean shoreline positions. (Top panel) Instantons mean shoreline positions and linear trends. (Middle panel) Deviation of mean shoreline positions from the linear trends. 30 days moving average filter is applied. (Bottom panel) Variation of 90 days cumulative cross shore energy flux C_{90}.

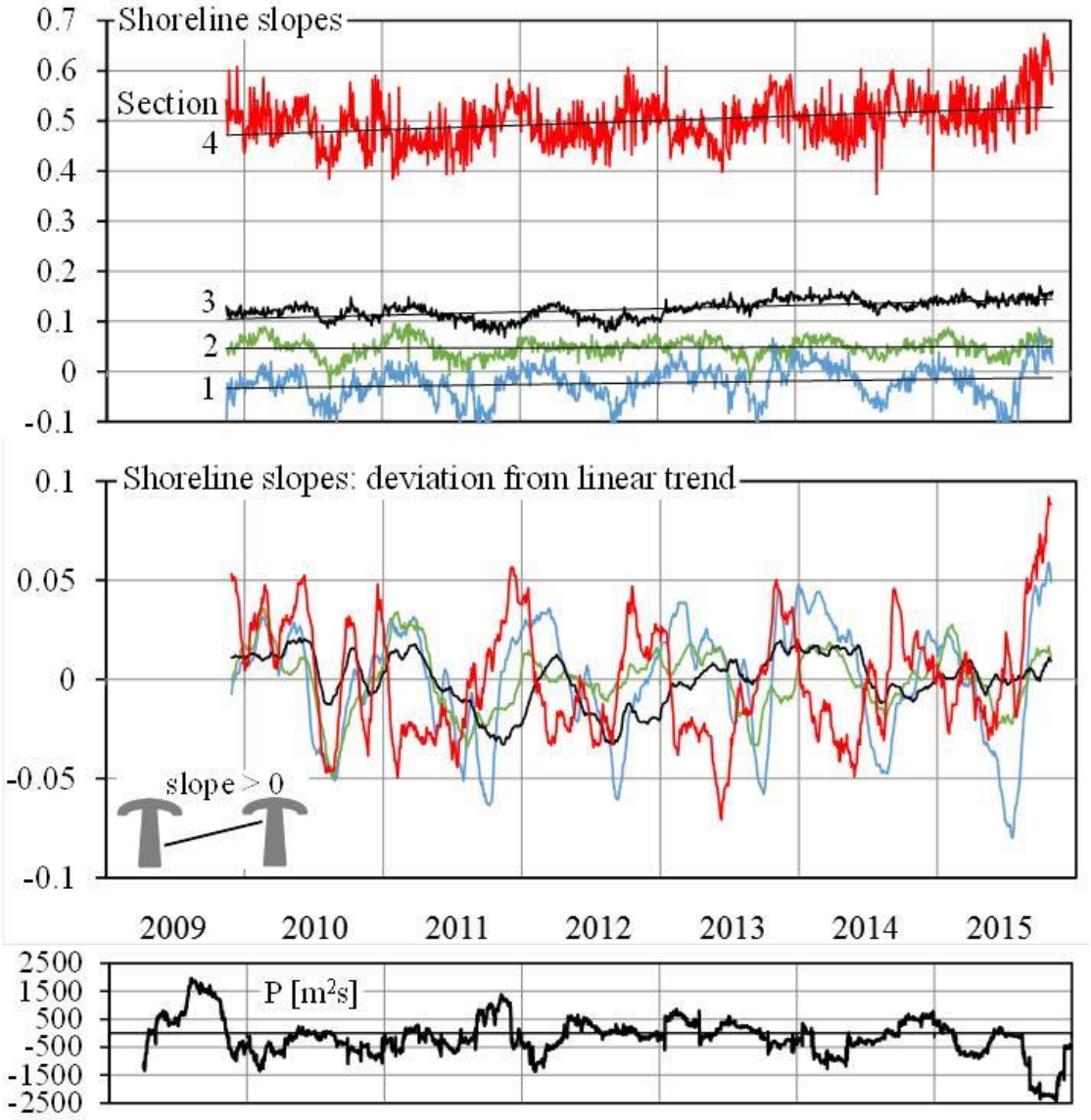

Figure 8. Variation of shoreline slopes. (Top panel) Instantons shoreline slopes and linear trends. (Middle panel) Deviation of shoreline slopes from the linear trends. 30 days moving average filter is applied. (Bottom panel) Variation of 90 days cumulative longshore energy flux (positive = southwards) P_{90}.

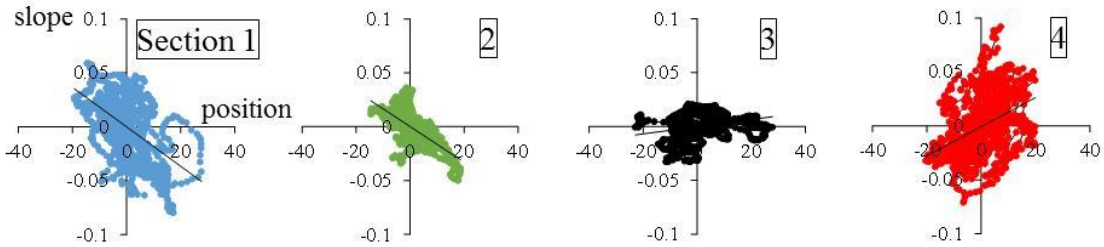

Figure 9. Scatter plots of deviations of shoreline position and shoreline slope at Sections 1 to 4.

2. Results

2.1. *Radar 1*

The beach of this area can be considered close to natural and undisturbed state. Elsayed and Takewaka (2016) have reported the results of 10 years observation. This portion is quite stable and there was no distinct trend in the variation of mean shoreline position. Figure 3 shows the variation of shoreline position at x = 500 m, which indicates that the shore is stable in the long-term, overlapped with seasonal fluctuations. Figure 4 displays the variation of overall shoreline positions of this area from 2005 to 2014.

In the previous study, the variation of shoreline position was split into two modes by Empirical Orthogonal Function analysis. The first mode was the almost longshore uniform and seasonal cross-shore movement of shoreline position, and the rest of the modes were small fluctuations propagating in the longshore. The latter can be seen as obliquely extending features in the Figure 4 (b). These are so-called shoreline features observed in the intertidal morphologies, and are migrating in the down-wave direction, southwards in winter and northwards in summer.

2.2. *Radar 2*

According to Banno et al (2017), mean shoreline position of the whole beach migrated remarkably in the past 50 years. This can be confirmed from the variation of shoreline position measured at x = 10,500 m as show in Figure 5. Shoreline shifted approximately 30 m to the seawards overlapped with seasonal fluctuations.

Figure 6 shows the overall shoreline positions measured with the Radar 2 from 2009 to 2015. It clearly shows, especially at the southern portion, that the shore is accumulating steadily resulting seawards shifts of shoreline positions. Since the sediment motions is restricted by the Headlands and jetty in this area, we discuss the characteristics of local beach change at the Sections 1 to 4, as shown in the diagram.

Mean shoreline positions of every section are shown in Figures 7. The mean shorelines are migrating seawards, especially at Sections 3 and 4 with a speed of order of 10 m per year. The seasonal fluctuations are derived by subtracting linear trend from the original data. They show basically a systematic variation except year 2011: in the summer, shoreline is shifting to the offshore, and in the winter, shoreline is retreating. In year 2011, accumulation in the summer was not observed, on the contrary, seawards shifts were observed in winter. A rough estimation to explain these behaviors, cross shore wave energy flux C was estimated from the wave record measured by the NOWPHAS of Kashima Port. The bottom panel of Figure 7 shows the variation of 90 days accumulated C_{90}. In the summer of 2011, C_{90} was relatively larger than other years, which is possible reason of smaller seawards shift of shoreline position.

Slope of shoreline distribution was estimated by linear fitting in every section. Figure 8 shows the variation of shoreline slopes, their linear trends and deviations from the linear trends. The shoreline slopes of this area are in increasing trend, especially at the Sections 3 and 4, which is accordant with the seawards shifts of the shorelines at these sections. The fluctuations of the slopes show different patterns: at the Sections 1 and 2, the deviations are basically negative in the summer, and positive in the winter seasons. This is due to southern incident waves in summer and northern waves in winter, respectively, which drive longshore sediments to the down-wave sides. The behavior, however, at the Sections 3 and 4 is different, and this can't be explained simply from the incident wave angles. Longshore shore wave energy flux P (positive: southwards) was estimated from the wave record measured by the NOWPHAS of Kashima Port. The bottom panel of Figure 8 shows the variation of 90 days accumulated P_{90}. Overall correlation between fluctuations of shoreline slopes and P_{90} are not clear, however, for limited periods, shoreline slopes increases accordingly with P_{90}.

Scatter plots of deviations of shoreline positions and slopes are shown in Figure 9, which shows clearly the sediment motions at Sections 1 and 2, and 3 and 4 are different. At Sections 1 and 2, the shoreline shifts seawards and northwards in the summer due to southern incident waves, and vice versa in winter. This is sometimes called as see-saw like shoreline change between jetties. On the contrary, at Section 4, an opposite pattern is observed. The southern incident waves are maybe sheltered and diffracted by the breakwater of the fishery port, resulting complex nearshore wave deformation and circulation, which needs further exploration.

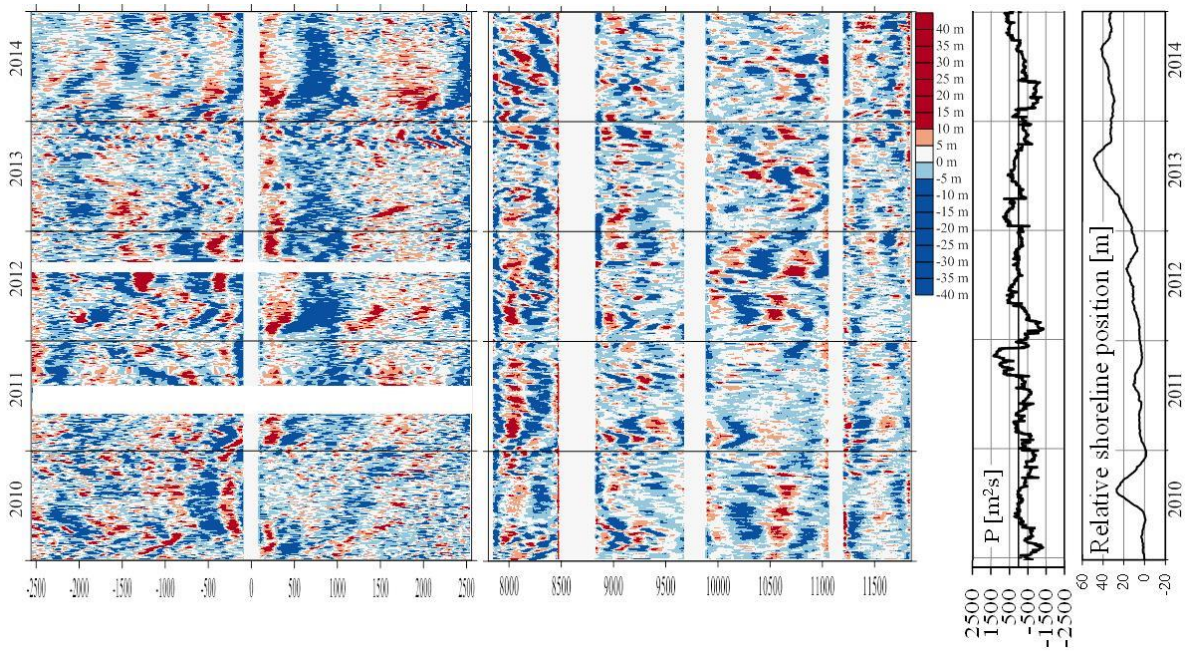

(a) Radar 1 (b) Radar 2 (c) (d)

Figure 10. Migrations of the wavy features observed in the shoreline positions. Lateral axis: longshore extent. Vertical axis: elapsed time. White belts indicate where data were not available. (a) Radar 1: At the research pier HORS. (b) Radar 2: At the southern end of littoral cell, (c) Variation of 90 days cumulative longshore energy flux (positive = southwards) P_{90}, and (d) Variation of relative mean shoreline position of $10000 < x < 11000$ m (Section 3).

2.3. *Longshore migrations of shoreline variabilities*

Inspecting carefully the variations of shoreline configurations, wavy features with wavelength of several hundred meters are frequently observed which are migrating to the down-wave at both radar sites. In the previous study (Elsayed and Takewaka, 2016), migration speeds showed high correlation with the longshore current velocities measured at the pier, suggesting that these migrations can be considered as signals of longshore sediments. Here we compare the migrations of the wavy features observed at two sites shown in Figures 10 (a) and (b). They show the temporal and spatial variations of local deviation of shoreline position, which is defined as the difference from the local spatial mean. Oblique patterns observed in both panels correspond to longshore migrations of wavy features: they mostly migrate to the southern in the winter and spring due to northern wave incidence, and vice versa in the rest of the seasons. Migration directions mostly coincide at the two radar sites, but their speeds (~ slopes of oblique features) are different: these can be partially correlated with the 90 days cumulative longshore wave energy flux as shown in Figure 10 (c). Figure 10 (d) sows the relative mean shoreline position of Section 3 ($10000 < x < 11000$ m). The interesting is the seawards shift of the shoreline position in 2013 is accompanied by distinct oblique pattern shown in panel (b). This is suggesting the migrations of wavy features can become a proxy of longshore sediment motion.

3. Concluding Remarks

In this observational study, details of the shoreline variations at two locations in a littoral cell are shown. One of the sites is close to a natural state and the other protected by coastal structures which limit longshore movement of the sediments.

Basically, in this area, shoreline positions shift seawards in the summer, and retreat in winter. At the end

of the cell, where the beach is protected by Headlands and a jetty, shoreline positions showed so called see-saw variation between the structures. Sediments moved to the down-wave, and shoreline slopes increased or decreased accordingly at the sections where the influence of the breakwater of the fishery port is small. On the contrary, at sections close to the breakwater of the fishery port, variation of shoreline slopes didn't follow the same manner. Detailed analyses on waves and currents are necessary to explain these different behaviors.

Inspecting carefully the variations of shoreline configurations, wavy features with wavelength of several hundred meters are frequently observed which are migrating to the down-wave at both radar sites. Most of the migrations seem to occur simultaneously, and their directions and speeds can be correlated partially with the longshore wave energy flux.

Acknowledgements

The radar observations are supported by the members of Littoral Drift Division, Port and Airport Research Institute. The result of the wave computations was provided by Dr. Elsayed Galal, Port Said University. This work is financially supported by the Grants-in-Aid of the Japan Society for the Promotion of Science (JSPS), and by the Social Implementation Program on Climate Change Adaptation Technology (SI-CAT), Ministry of Education, Culture, Sports, Science and Technology.

References

Banno, M., Takewaka S. and Kuriyama Y., 2017, Multidecadal shoreline evolution due to large-scale beach nourishment –Japanese sand engine? -, *Coastal Dynamics 2017*.

Elsayed, M. G., and Takewaka, S., 2015, Temporal and spatial shoreline variability observed with a X-band radar at Hasaki Coast, Japan, *Coastal Sediments 2015*, ASCE.